

An X-Band 300-Watt Class High Power GaN HEMT Amplifier for Radar Applications

Ken KIKUCHI*, Makoto NISHIHARA, Hiroshi YAMAMOTO, Shinya MIZUNO, Fumikazu YAMAKI and Takashi YAMAMOTO

A high-output power and broadband GaN high electron mobility transistor (HEMT) has been developed for X-band applications. The device consists of 2-dice of 14.4-millimeter gate periphery together with input and output 2-stage impedance transformers. The device exhibited saturated output power of 310 W with power gain of 10.0 dB over the wide frequency range of 8.5-10.0 GHz, operating at 65 V drain voltage under pulsed condition. In addition, the highest saturated output power reached 333 W with power gain of 10.2 dB at 9.0 GHz. This is the highest output power GaN HEMT ever reported for X-band.

Keywords: GaN HEMT, Amplifier, X-band, Radar, High-Output Power

1. Introduction

Recently, a gallium nitride high electron mobility transistor (GaN HEMT) has been developed for X-band applications such as marine and meteorological radars. A placement of large number of small meteorological radars in an urban area enables the detection of a local change in the weather. Therefore the meteorological radar market is expected to grow due to the replacement of obsolete radar components with GaN HEMT.

For X-band radar applications, traveling wave tubes (TWT) such as magnetrons and klystrons were conventionally used because of the required power level as high as 1 kilowatt. However, it is pointed out that TWT amplifiers have high maintenance costs due to their short lifespan. Moreover, TWT amplifiers produce large signal noise and occupy large bandwidth, they interfere with other wireless communication systems running in an adjacent band. Consequently, there is a strong desire for solid-state power amplifiers (SSPA) that are superior in long-term reliability and signal noise to replace conventional TWT amplifiers.

GaN HEMT has attracted much attention as a candidate for SSPA devices because of its excellent capabilities such as high power, high efficiency and high gain with high voltage operation based on the excellent material properties of GaN. In addition, the GaN HEMT is capable of covering wide bandwidth due to its high input and output impedance.

Sumitomo Electric Industries, Ltd. and its wholly owned subsidiary Sumitomo Electric Device Innovations, Inc. were the first in the world to have started mass production and received the Technology Management & Innovation Award 2013.⁽¹⁾ Based on our well-established L-/S-band GaN HEMT technology⁽²⁾ we have pursued the enhancement of output power and bandwidth of internally-matched GaN HEMT power amplifier for X-band radar applications.^{(3),(4)} This paper introduces our work on the development of internally-matched GaN HEMT power amplifier with the world's highest output power and widest bandwidth.

2. GaN HEMT Technology

2-1 Material properties

Table 1 shows the key material parameters of major semiconductor materials used in high frequency applications. GaN has a saturated electron velocity (V_{sat}) twice as high as that of Si or GaAs, and a critical breakdown field (E_c) 10 times and 7.5 times larger than those of Si and GaAs, respectively. Additionally, Johnson's figure of merit (JFOM) of GaN is 27 times higher than that of Si and 15 times higher than that of GaAs. JFOM, expressed as $V_{sat} \cdot E_c / 2 \Pi$, is a common benchmark for the performance of high frequency and high power devices.

Table 1. Material parameters comparison

	Si	GaAs	SiC	GaN
Band gap energy (eV)	1.1	1.4	3.2	3.4
Saturated velocity ($\times 10^7$ cm/s)	1.0	1.3	2.0	2.7
Critical breakdown field (MV/cm)	0.3	0.4	3.0	3.0
Mobility ($\text{cm}^2/\text{V}\cdot\text{s}$)	1300	6000	600	1500
Thermal conductance ($\text{W}/\text{cm}\cdot\text{K}$)	1.5	0.5	4.9	1.5
JFOM versus Si	1.0	1.7	20	27

2-2 GaN HEMT structures

The epitaxial layers of the GaN HEMT grown on a semi-insulating SiC substrate are ideal for high power devices from a viewpoint of thermal management due to the good thermal conductivity of SiC. In addition, the additive effects of spontaneous polarization and piezo polarization, which are characteristic properties of GaN crystals, can generate 2DEG (two-dimensional electron

gas) on the order of 10^{13} cm^{-2} . Therefore, the GaN HEMT promises more than 10 times higher output power than GaAs devices with the same gate width. The gate length is optimized to obtain sufficient power gain for X-band radar applications.

Figure 1 shows the drain current-voltage (I_{ds} - V_{ds}) characteristics of the fabricated GaN HEMT. We obtained high maximum drain current of 1.1 A/mm at a gate voltage (V_{gs}) of +2.0 V with high BV_{dsx} of 290 V. Our previous study showed that the BV_{dsx} of four times that of the operation drain voltage is required to secure a reliable operation.⁽⁵⁾ The BV_{dsx} of 290 V is sufficient for 65 V operation.

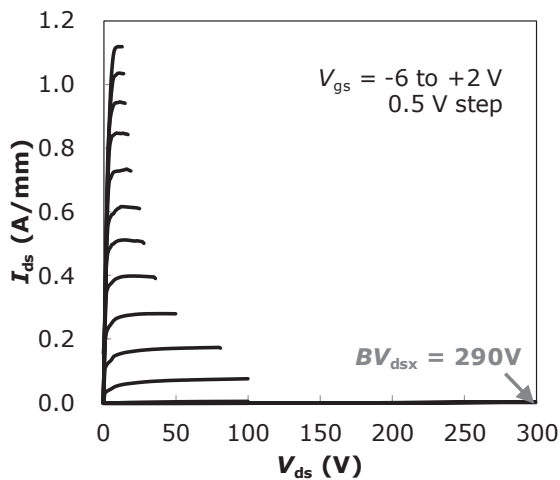


Fig. 1. I_{ds} - V_{ds} characteristics of the GaN HEMT

3. Examination of Broadband Design

3-1 Limitation of bandwidth

The target bandwidth was set to be the 8.5-10.0 GHz frequency range which covers most X-band applications. The fractional bandwidth is calculated to be 0.16.

Figure 2 shows the simplified schematic diagram of the impedance-matching circuit in the output-matching network for transistors. As shown in **Fig. 2**, the drain-to-source capacitance (C_{ds}) of transistors is connected in parallel with the drain-to-source resistance (R_{ds}). To obtain both high-output power and wide bandwidth, two possible limiting factors need to be considered⁽⁶⁾: Q-factor and output impedance (Z_{out}) of a transistor. The former, theoretically investigated by Fano,⁽⁷⁾ gives the gain-bandwidth matching restriction for the ideal case of a lossless matching network. As for the latter limitation, Matthaei has reported a relationship between impedance-transformation ratio and fractional bandwidth at a certain attenuation condition of a filter.⁽⁸⁾ Since an internally-matched power amplifier has a restriction of the number of impedance transformers due to its size limitation, the number of trans-

forming stages and the impedance-transformation ratio limits the fractional bandwidth. Here, the impedance transformation ratio (r) is defined as $r = 50/Z_{out}$.

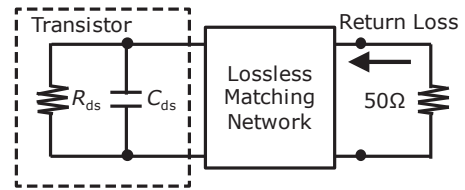


Fig. 2. Schematic diagram of lossless impedance matching network including transistor's parasitic reactance

3-2 Q-factor

According to Fano's theory, i.e. the former limitation, the fractional bandwidth of the circuit BW_{Fano} is given by

$$BW_{Fano} = \frac{-\pi}{Q \times \ln(|\Gamma|)} \dots\dots\dots (1)$$

$$Q = \omega_c R_{ds} C_{ds} \dots\dots\dots (2),$$

where Q , Γ , and ω_c denote Q-factor, reflection coefficient, and center angular frequency, respectively. **Figure 3** shows the dependence on the Q-factor of fractional bandwidth BW_{Fano} . The VSWR is set to be 1.5. As shown in **Fig. 3**, to obtain the target fractional bandwidth of 0.16, Q-factor must be 12.3 or below.

3-3 Impedance transformation ratio

Matthaei has presented a design theory for the synthesis of lumped-element Chebyshev impedance-transforming networks and has shown attainable fractional bandwidth BW_{Zout} with respect to the impedance-transformation ratio with a finite number of transformers.⁽⁹⁾ The estimated fractional bandwidth against the impedance-transformation ratio with 1- and 2-stage transformers is shown in **Figure 4**. The target fractional bandwidth can be obtained without restriction of impedance-transformation ratio in case of 2-stage transformers. These results indicate that the target fractional bandwidth is achievable as long as the Q-factor is optimized in the device with 2-stage transformers.

The fabricated device parameters are summarized in **Table 2**. The Q-factor and impedance-transformation ratio were obtained from S-parameter and load-pull measurements, respectively. These measurements were performed with a 0.9-millimeter GaN HEMT, and the parameters were transformed to that of 28.8-millimeter GaN HEMT. The obtained Q-factor of 12.2 satisfies the requirement for target fractional bandwidth. The impedance-transformation ratio is also acceptable. Since the obtained impedance-transformation ratio is insufficient for target fractional bandwidth with 1-stage transformers, we selected 2-stage transformers.

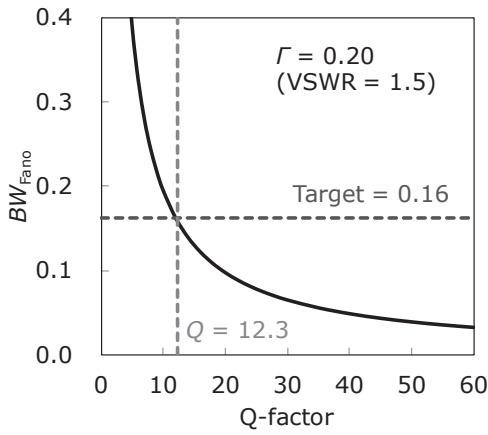


Fig. 3. Estimated dependence on the Q-factor of fractional bandwidth

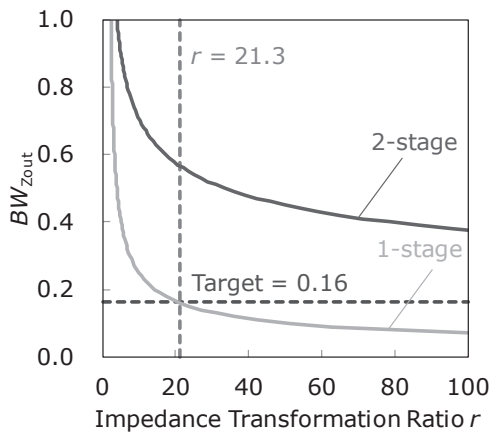


Fig. 4. Estimated dependence on the impedance-transformation ratio of fractional bandwidth

Table 2. Parameters of fabricated device

R_{ds} (Ω)	C_{ds} (pF)	Q	Z_{out} (Ω)	r
23.8	8.9	12.2	0.69	72.8

4. Matching Circuit Design

Figure 5 shows the top view of the developed device. The unit gate width and gate periphery are $150 \mu\text{m}$ and 14.4 mm , respectively. The dice size is $5.38 \text{ mm} \times 0.76 \text{ mm}$. Two dice of GaN HEMT together with internal matching circuits were mounted in a ceramic-metal package. The package with a low thermal resistance base plate is used in order to achieve a maximum thermal diffusion, giving lower thermal resistance. The package size is $24.0 \text{ mm} \times 17.4 \text{ mm}$. The impedance of both input and output ports were designed to be 50Ω .

Figure 6 shows the circuit network of the developed device. The output-matching circuit consisting of two stages of a transmission line was designed to match maximum output power. This matching imped-

ance was measured by load-pull method. Harmonic impedances are not controlled in this matching circuit design, which limits the efficiency.

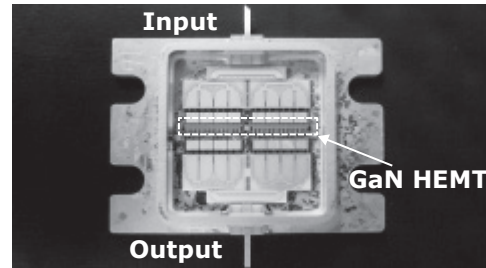


Fig. 5. Top view of the developed device

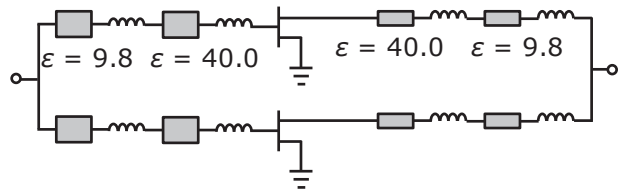


Fig. 6. Schematic diagram of circuit network

5. RF Performance

Figure 7 shows the measured operating drain voltage dependence of the output power (P_{out}) and linear gain (G_L) at 9.0 GHz under pulsed condition. The duty cycle of the pulse is 10% with a pulse width of $100 \mu\text{sec}$. The output power and the linear gain increase with V_{ds} , and each maximum value was obtained at V_{ds} of 65 V .⁽⁹⁾

Figure 8 shows the output power, power-added-efficiency (PAE) and gain versus input power (P_{in}) at a drain voltage of 65 V and frequency of 9.0 GHz . Saturated output power (P_{sat}) of 333 W , power gain (G_p) of 10.2 dB and PAE of 37% were obtained under the same pulsed condition.⁽¹⁰⁾

Figure 9 shows the broadband RF performance over the $8.5\text{--}10.0 \text{ GHz}$ frequency range measured under the same pulsed condition. The device exhibited excellent broadband capability of 16% fractional bandwidth with P_{sat} of 310 W and G_p of 10.0 dB .⁽⁹⁾

Table 3 summarizes the measurement results of the developed internally-matched GaN HEMT power amplifier. The developed device exhibited saturated output power of 310 W with power gain of 10.0 dB over the wide frequency range of $8.5\text{--}10.0 \text{ GHz}$. In addition, the highest saturated output power reached 333 W with a power gain of 10.2 dB at 9.0 GHz . These results show the highest output power of GaN HEMT ever reported for X-band.

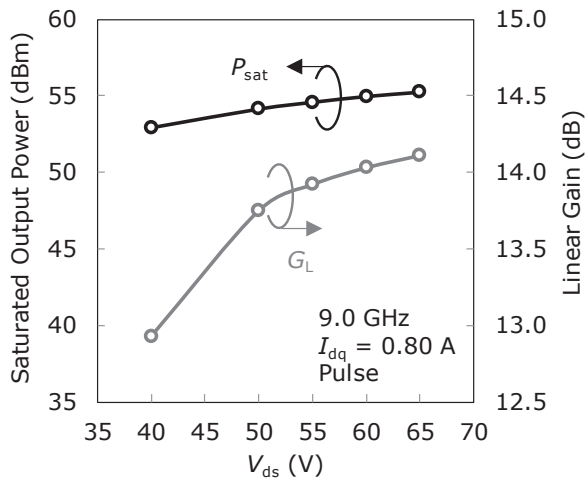


Fig. 7. Drain voltage dependence of P_{out} and G_L

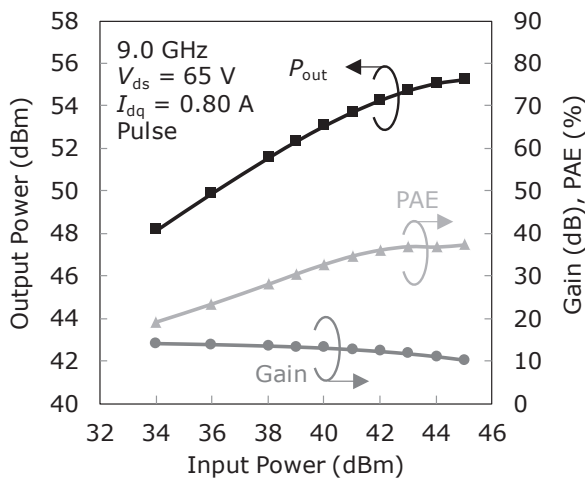


Fig. 8. P_{in} vs. P_{out} characteristics of developed device

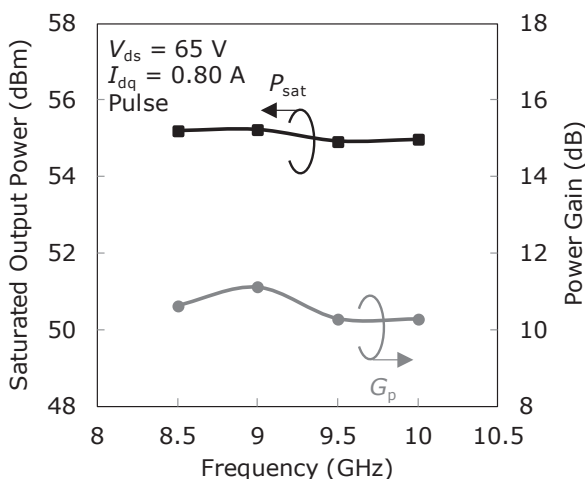


Fig. 9. Frequency response of the developed device

Table 3. Measurement results of developed device

Parameters	Results
Drain voltage V_{ds}	65 V
Pulse width	100 μ sec
Duty	10%
Frequency (full bandwidth)	8.5-10.0 GHz
Saturated output power P_{sat}	54.9 dBm (310 W)
Power gain G_p	10.0 dB
Frequency (Maximum P_{sat})	9.0 GHz
Saturated output power P_{sat}	55.2 dBm (333 W)
Power gain G_p	10.2 dB
Power added efficiency PAE	37%

6. Conclusion

In X-band radar applications, the downsizing and enhancement of long-term reliability of the system by the replacement of TWT amplifiers with SSPA are strongly recommended. In this study, we have developed an internally-matched GaN HEMT power amplifier with world's highest output power and broadband capability ever reported in X-band. These results prove that our device is appropriate SSPA for X-band radar applications. We continue to develop even higher power and higher frequency GaN HEMT devices.

References

- (1) URL http://global-sei.com/news/press/14/prs010_s.html
- (2) K. Inoue, S. Sano, Y. Tateno, F. Yamaki, K. Ebihara, N. Ui, A. Kawano, H. Deguchi, "Development of Gallium Nitride High Electron Mobility Transistors for Cellular Base Stations," SEI technical review, No. 71, pp.88-93 (October 2010)
- (3) T. Yamamoto, E. Mitani, K. Inoue, M. Nishi, and S. Sano, "A 9.5-10.5 GHz 60 W AlGaIn/GaN HEMT for X-band High Power Application," Proc. Eur. Microw. Integr. Circuits Conf., pp. 173-175, Munich, Germany (October 2007)
- (4) M. Nishihara, T. Yamamoto, S. Mizuno, S. Sano, and Y. Hasegawa, "X-band 200W AlGaIn/GaN HEMT for high power application," Proc. Eur. Microw. Integr. Circuits Conf., pp. 65-68, Manchester, UK (October 2011)
- (5) F. Yamaki, K. Inoue, M. Nishi, H. Haematsu, N. Ui, K. Ebihara, A. Nitta, and S. Sano, "Ruggedness and Reliability of GaN HEMT," Proc. Eur. Microw. Integr. Circuits Conf., pp. 328-331, Manchester, UK (October 2011)
- (6) S. Mizuno, F. Yamada, H. Yamamoto, M. Nishihara, T. Yamamoto, and S. Sano, "A 5.9-8.5 GHz 20 Watts GaN HEMT," Proc. Asia-Pacific Microwave Conf., pp. 123-126, Yokohama, Japan (December 2010)
- (7) R. M. Fano, "Theoretical limitations on the broadband matching of arbitrary impedance," J. of Franklin Inst., vol. 249, pp. 57-84 and pp. 139-154 (Jan.-Feb. 1950)
- (8) G. L. Matthaei, "Tables of Chebyshev impedance-transforming networks of low-pass filter form," Proceedings of IEEE, pp. 939-963 (December 1964)

- (9) K. Kikuchi, M. Nishihara, H. Yamamoto, S. Mizuno, F. Yamaki and T. Yamamoto, "A 65 V operation high power X-band GaN HEMT amplifier," Proc. Asia-Pacific Microwave Conf., pp. 585-587, Sendai, Japan (November 2014)
- (10) K. Kikuchi, M. Nishihara, H. Yamamoto, S. Mizuno, F. Yamaki, T. Yamamoto and S. Sano, "An 8.5-10.0 GHz 310 W GaN HEMT for Radar Applications," IEEE MTT-S Int. Microwave Symp. Dig., pp. 1-4, Tampa, USA (June 2014)

Contributors (The lead author is indicated by an asterisk (*).)

K. KIKUCHI*

- Transmission Devices Laboratory



M. NISHIHARA

- Electron Devices Division, Sumitomo Electric Device Innovations, Inc.



H. YAMAMOTO

- Ph. D.
Electron Devices Division, Sumitomo Electric Device Innovations, Inc



S. MIZUNO

- Electron Devices Division, Sumitomo Electric Device Innovations, Inc.



F. YAMAKI

- Manager, Electron Devices Division, Sumitomo Electric Device Innovations, Inc.



T. YAMAMOTO

- Senior Manager, Electron Devices Division, Sumitomo Electric Device Innovations, Inc.

